# Speed-Sensorless Predictive Current Control for a Dual Three-phase Induction Machine Using a Kalman Filter for Electrial Vehicle Applications

Osvaldo Gonzalez*, Magno Ayala*, Jorge Rodas*, Raul Gregor* and Jesus Doval-Gandoy[†]

*Laboratory of Power and Control Systems, Facultad de Ingeniería, Universidad Nacional de Asunción, Paraguay

E-mail: {ogonzalez, mayala, jrodas & rgregor}@ing.una.py

[†]Applied Power Electronics Technology Research Group, University of Vigo, Spain

E-mail: jdoval@uvigo.es

*Abstract*—For a electrical application involving induction machines, such as the electrical propulsion drive of an electric vehicle, the rotor current cannot be measured, so it must be estimated. This paper describes the rotor current estimation through reduced order estimator known as Kalman filter to apply a sensorless speed control of dual three-phase induction machines by using an inner loop of model-based predictive control. Finally, simulation results are provided to show the efficiency of the proposed sensorless speed control algorithm, thus concluding that the system can work properly without the speed sensor.

*Index Terms*—Electric vehicle, multiphase machine, predictive control, sensorless control, Kalman filter.

## I. INTRODUCTION

In the last decade, the interest in multiphase machines has risen due to intrinsic features such as lower torque ripple, power splitting or better fault tolerance than three-phase machines. Recent research works and developments support the prospect of future more widespread applications of multiphase machines. In recent times, some of the applications of multiphase machines are being studied, such as electric vehicles (EV) and railway traction, all-electric ships, more-electric aircraft, and wind power generation systems [1].

EV is a road vehicle which involves an electric propulsion system. With this broad definition in mind, EVs may include battery electric vehicles, hybrid electric vehicles and fuelcell electric vehicles. The propulsion drive of an EV basically consists of a battery, an electronic converter, an electric motor, and a speed and/or torque sensor. Considering multiphase machines as the electrical motor has several advantages, i.e. fault tolerance and higher reliability, and the higher power splitting across the different phases [2]. Due to the benefits of multiphase machines it can be applied in propulsion applications, like more electric aircraft [3], electrical and hybrid vehicles [4].

For controlling the variables of dual three-phase induction machines (DTPIM), the most used methods are the direct torque control (DTC) and the vector control using an inner loop current control [5]. However, DTC has some problems such as: weakness in torque control at very low speed, torque and flux pulsations due to the hysteresis bands in

comparators, and variable frequency behavior [6]. On the other hand, field oriented control (FOC) or vector control is known for its good current behavior, but it contains one speed control loop, one flux control loop, four current control loops and some transformation models for different coordinate frames. Therefore, the cost and complexity of the system is increased. Compared to FOC, model predictive control (MPC) is very intuitive and easy to implement. Predictive current control (PCC) is an important branch of Finite-State MPC. Currents are controlled with a high precision, whereas the system dynamic performance is also very well [7]. There are very active research areas focused on the development of speed sensorless control strategies due to their advantages compared to the conventional control techniques such as elimination of direct sensor wiring, better noise immunity, lower cost, increased reliability and less maintenance requirement [5]–[7].

Although speed sensorless operation of a three-phase induction machines is already well developed, little work has been conducted for multiphase induction machines [8]. Besides, some of the control loops on the MPC have unmeasured variables, such as rotor current, so a state observer is required [9]. The observers are mainly classified into two groups: deterministic observers such as Luenberger observer (LO) [5], model reference adaptive system (MRAS) [10], sliding mode observer (SMO) [11] and stochastic observer such as Kalman filter (KF) [9], being the KF the best choice to obtain high-accuracy estimates of dynamic system states [12].

This paper considers the sensorless speed control of DTPIM for EVs by using an inner loop of MPC, to predict the effects of future control actions on the state variables. In order to achieve this goal, the proposed algorithm uses reduced order estimators based on a KF to estimate the rotor current. Thereafter the rotor current estimated is used to determine an estimate of the speed of the machine. The performance of the proposed control technique in a DTPIM drive is studied for varying load operations and varying speeds.

This paper is organized as follows. Section II describes the DTPIM drive, Section III presents the mathematical model of the machine, Section IV details the predictive model with the speed observer and the current control with rotor current
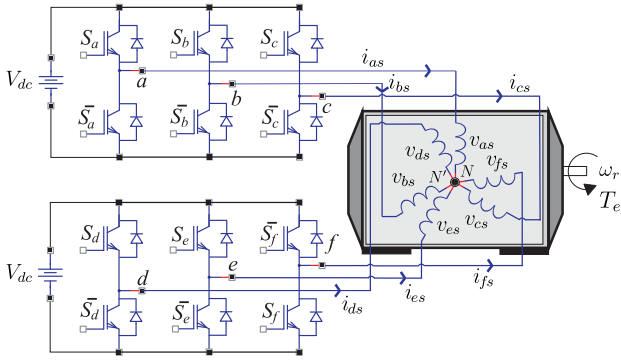
Fig. 1. A general scheme of a dual three-phase induction machine.



Fig. 2. Voltage space vectors and switching states in the $(\alpha-\beta)$ and $(x-y)$ subspaces for a dual three-phase VSI.

estimator based on KF and presents the proposed predictive control method for the dual three-phase induction machine. Simulation results are provided in Section V, showing the efficiency obtained by speed estimator. The conclusions are finally summarized in the last section.

## II. THE DUAL THREE-PHASE INDUCTION MACHINE DRIVE

The system under study consists of an DTPIM fed by a dual three-phase VSI and a dc link. A detailed scheme of the drive is provided in Fig. 1.

This DTPIM is a continuous system which can be described by a set of differential equations. The model of the system can be simplified by means of the vector space decomposition (VSD) introduced in [13]. Thus, the original six-dimensional space of the machine is transformed into three two-dimensional orthogonal subspaces in the stationary reference frame $(\alpha-\beta)$, $(x-y)$ and $(z_1-z_2)$. This transformation is obtained through a 6 x 6 transformation matrix:

$$\mathbf{T} = \frac{1}{3} \begin{bmatrix} 1 & \frac{\sqrt{3}}{2} & -\frac{1}{2} & -\frac{\sqrt{3}}{2} & -\frac{1}{2} & 0 \\ 0 & \frac{1}{2} & \frac{\sqrt{3}}{2} & \frac{1}{2} & -\frac{\sqrt{3}}{2} & -1 \\ 1 & -\frac{\sqrt{3}}{2} & -\frac{1}{2} & \frac{\sqrt{3}}{2} & -\frac{1}{2} & 0 \\ 0 & \frac{1}{2} & -\frac{\sqrt{3}}{2} & \frac{1}{2} & \frac{\sqrt{3}}{2} & -1 \\ 1 & 0 & 1 & 0 & 1 & 0 \\ 0 & 1 & 0 & 1 & 0 & 1 \end{bmatrix} \quad (1)$$

where an amplitude invariant criterion was used.

For a machine with distributed windings, the $(\alpha-\beta)$ components contributes to useful power conversion (i.e. flux and torque production), while the $(x-y)$ and $(z_1-z_2)$ components only result in losses and are usually minimized, except during post-fault operations. For two isolated neutrals configuration, both $(z_1-z_2)$ currents cannot flow, so the $(z_1-z_2)$ components can be ignored [14].

The VSI has a discrete nature, actually, it has a total number of $2^6 = 64$ different switching states defined by six switching functions corresponding to the six inverter legs $[S_a, S_b, S_c, S_d, S_e, S_f]$, where $\mathbf{S}_i \in \{0, 1\}$. The different switching states and the voltage of the DC link (Vdc) define the phase voltages which can in turn be mapped to the $(\alpha-\beta)-(x-y)$ space according to the VSD approach. For this reason, the 64 different on/off combinations of the six
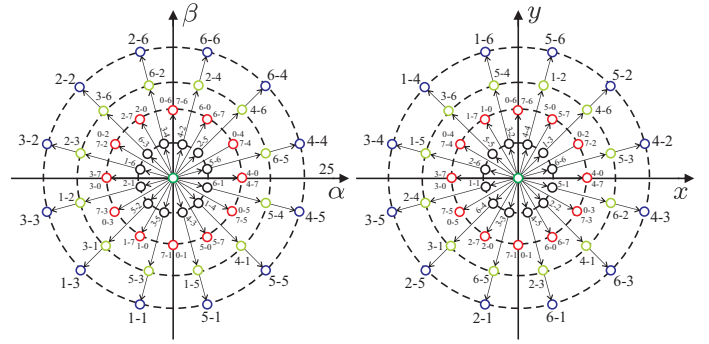
VSI legs lead to 64 space vectors in the $(\alpha-\beta)$ and $(x-y)$ subspaces. Fig. 2 shows the active vectors in the $(\alpha-\beta)$ and $(x-y)$ subspaces, where each vector switching state is identified using the switching function by two octal numbers corresponding to the binary numbers $[S_a S_c S_e]$ and $[S_b S_d S_f]$, respectively.

As it is shown in Fig. 2 the 64 possibilities lead to only 49 different vectors in the $(\alpha-\beta)-(x-y)$ subspace. On the other hand, a transformation matrix must be used to represent the stationary reference frame $(\alpha-\beta)$ in the dynamic reference $(d-q)$. This matrix is given by:

$$\mathbf{T}_{dq} = \begin{bmatrix} cos(\delta_r) & -sin(\delta_r) \\ sin(\delta_r) & cos(\delta_r) \end{bmatrix} \quad (2)$$

where $\delta_r$ is the rotor angular position referred to the stator.

## III. MACHINE MODEL

It is possible to model the machine by using an state-space representation, based on the VSD approach and the dynamic reference transformation. This model is given by:

$$\frac{d}{dt}\mathbf{X}_{\alpha\beta xy} = \mathbf{A}\mathbf{X}_{\alpha\beta xy} + \mathbf{B}\mathbf{U}_{\alpha\beta xy}$$
$$\mathbf{Y}_{\alpha\beta xy} = \mathbf{C}\mathbf{X}_{\alpha\beta \mathbf{xy}} \quad (3)$$

where $\mathbf{U}_{\alpha\beta xy} = \begin{bmatrix} u_{\alpha s} & u_{\beta s} & u_{xs} & u_{ys} & 0 & 0 \end{bmatrix}^T$ represents the input vector of the system, $\mathbf{X}_{\alpha\beta xy} = \begin{bmatrix} i_{\alpha s} & i_{\beta s} & i_{xs} & i_{ys} & i_{\alpha r} & i_{\beta r} \end{bmatrix}^T$ denotes the state vector, $\mathbf{Y}_{\alpha\beta xy} = \begin{bmatrix} i_{\alpha s} & i_{\beta s} & i_{xs} & i_{ys} & 0 & 0 \end{bmatrix}^T$ indicates the output vector and $\mathbf{A}$, $\mathbf{B}$ and $\mathbf{C}$ are matrices that define the dynamics of the electrical drive.

The mechanical part of the electrical drive is given by the following equations:

$$T_e = 3P(\psi_{\alpha s}i_{\beta s} - \psi_{\beta s}i_{\alpha s}) \quad (4)$$

$$J_i\frac{d}{dt}\omega_r + B_i\omega_r = P(T_e - T_L) \quad (5)$$

where $T_L$ denotes the load torque, $T_e$ is the generated torque, $J_i$ the inertia coefficient, $P$ the number of pairs of poles, $\psi_{\alpha\beta s}$ the stator flux, $B_i$ the friction coefficient and $\omega_r$ is the rotor angular speed.

## IV. PREDICTIVE MODEL

Assuming the mathematical model expressed by (3) and using the state variables defined by the vector $\mathbf{X}_{\alpha\beta xy}$, we can define the following set of equations:

$$\frac{d}{dt}(x_1) = -R_s c_2 x_1 + c_4 \left(L_m \omega_r x_2 + R_r x_5 + L_r \omega_r x_6\right) + c_2 u_1$$

$$\frac{d}{dt}(x_2) = -R_s c_2 x_2 + c_4 \left(-L_m \omega_r x_1 - L_r \omega_r x_5 + R_r x_6\right) + c_2 u_2$$

$$\frac{d}{dt}(x_3) = -R_s c_3 x_3 + c_3 u_3$$

$$\frac{d}{dt}(x_4) = -R_s c_3 x_4 + c_3 u_4$$

$$\frac{d}{dt}(x_5) = -R_s c_4 x_1 + c_5 \left(-L_m \omega_r x_2 - R_r x_5 - L_r \omega_r x_6\right) - c_4 u_1$$

$$\frac{d}{dt}(x_6) = -R_s c_4 x_2 + c_5 \left(L_m \omega_r x_1 + L_r \omega_r x_5 - R_r x_6\right) - c_4 u_2 \tag{6}$$

where $R_s$, $L_s = L_{ls} + L_m$, $R_r$, $L_r = L_{lr} + L_m$ and $L_m$ are the electrical parameters of the machine and the coefficients $c_i$ for $i = 1, \ldots, 5$, are defined as $c_1 = L_s L_r - L_m^2$, $c_2 = \frac{L_r}{c_1}$, $c_3 = \frac{1}{L_{ls}}$, $c_4 = \frac{L_m}{c_1}$ y $c_5 = \frac{L_s}{c_1}$, while the input vector corresponds to the voltages applied to the stator $u_1 = v_{\alpha s}$, $u_2 = v_{\beta s}$, $u_3 = v_{xs}$, $u_4 = v_{ys}$ and the state vector corresponds to the DPTIM currents $x_1 = i_{\alpha s}$, $x_2 = i_{\beta s}$, $x_3 = i_{xs}$, $x_4 = i_{ys}$, $x_5 = i_{\alpha r}$ and $x_6 = i_{\beta r}$.

Stator voltages are related to the input control signals through the inverter model. In this case, the simplest model, used for isolated neutral configuration, has been considered for the sake of speeding up the optimization process. Then if the gating signals are arranged in the vector $\mathbf{S} = [S_a, S_b, S_c, S_d, S_e, S_f]$, where the stator voltages can be obtained from:

$$\mathbf{M} = \frac{1}{3} \begin{bmatrix} 2 & 0 & -1 & 0 & -1 & 0 \\ 0 & 2 & 0 & -1 & 0 & -1 \\ -1 & 0 & 2 & 0 & -1 & 0 \\ 0 & -1 & 0 & 2 & 0 & -1 \\ -1 & 0 & -1 & 0 & 2 & 0 \\ 0 & -1 & 0 & -1 & 0 & 2 \end{bmatrix} \cdot \mathbf{S}^T \tag{7}$$

An ideal inverter converts gating signals into stator voltages that can be projected to $(\alpha - \beta)$ and $(x - y)$ subspaces and gathered in a row vector $\mathbf{U}_{\alpha\beta xy}$ computed as:

$$\mathbf{U}_{\alpha\beta xy} = [u_{\alpha s}\ u_{\beta s}\ u_{xs}\ u_{ys}\ 0\ 0]^T = V dc \cdot \mathbf{T} \cdot \mathbf{M} \tag{8}$$

being $V dc$ the dc link voltage and the superscript $(^T)$ indicates the transposed matrix. Applying the rotational transformation (2) to the $(\alpha - \beta)$ components, we can obtain:

$$\mathbf{U}_{dq} = [u_{ds}\ u_{qs}]^T = \mathbf{T}_{dq} \cdot \begin{bmatrix} u_{\alpha s} \\ u_{\beta s} \end{bmatrix} \tag{9}$$

By combining the equations (6)-(9) a nonlinear set of equations arises that can be written in state space form:

$$\dot{\mathbf{X}}_{(t)} = f\left(\mathbf{X}_{(t)}, \mathbf{U}_{(t)}\right)$$
$$\mathbf{Y}_{(t)} = \mathbf{C}\mathbf{X}_{(t)} \tag{10}$$

with state vector $\mathbf{X}_{(t)} = [x_1, x_2, x_3, x_4, x_5, x_6]^T$, input vector $\mathbf{U}_{(t)} = [u_1, u_2, u_3, u_4]$, and $\mathbf{Y}_{(t)} = [x_1, x_2, x_3, x_4]^T$ as the output vector. The components of the vectorial function $f$ and the matrix $\mathbf{C}$ are obtained in a straightforward manner from (6) and the definitions of state and output vector. Model (10) must be discretized in order to be of used for the predictive controller. A forward Euler method is used to keep a low computational cost. Due to this fact, the resulting equations will have the required digital control form, with predicted variables depending just on past values and not on present values of the variables. Thus, a prediction of the future next-sample state $\hat{\mathbf{X}}_{[k+1|k]}$ is expressed as:

$$\hat{\mathbf{X}}_{[k+1|k]} = \mathbf{X}_{[k]} + T_m f\left(\mathbf{X}_{[k]}, \mathbf{U}_{[k]}, \omega_{r[k]}\right) \tag{11}$$

where $[k]$ is the current sample and $T_m$ the sampling time.

### A. Reduced order estimators

In the state space description (10) only stator currents, voltages and mechanical speed are measured. Stator voltages are easily predicted from the gating commands issued to the VSI, rotor current, however, cannot be directly measured. This difficulty can be overcome by means of estimating the rotor current using the concept of reduced order estimators.

The reduced order estimators provide an estimate for only the unmeasured part of the state vector, then, the evolution of states can be written as:

$$\underbrace{\begin{bmatrix} \hat{\mathbf{X}}_{a[k+1|k]} \\ \hat{\mathbf{X}}_{b[k+1|k]} \\ \hat{\mathbf{X}}_{c[k+1|k]} \end{bmatrix}}_{[\hat{\mathbf{X}}_{[k+1|k]}]} = \underbrace{\begin{bmatrix} \overline{\mathbf{A}}_{11} & \overline{\mathbf{A}}_{12} & \overline{\mathbf{A}}_{13} \\ \overline{\mathbf{A}}_{21} & \overline{\mathbf{A}}_{22} & \overline{\mathbf{A}}_{23} \\ \overline{\mathbf{A}}_{31} & \overline{\mathbf{A}}_{32} & \overline{\mathbf{A}}_{33} \end{bmatrix}}_{[\mathbf{A}]} \underbrace{\begin{bmatrix} \mathbf{X}_{a[k]} \\ \mathbf{X}_{b[k]} \\ \mathbf{X}_{c[k]} \end{bmatrix}}_{[\mathbf{X}_{[k]}]} \tag{12}$$
$$+ \underbrace{\begin{bmatrix} \overline{\mathbf{B}}_1 \\ \overline{\mathbf{B}}_2 \\ \overline{\mathbf{B}}_3 \end{bmatrix}^T}_{[\mathbf{B}]} \underbrace{\begin{bmatrix} \mathbf{U}_{\alpha\beta s} \\ \mathbf{U}_{xys} \\ \mathbf{U}_{\alpha\beta s} \end{bmatrix}}_{[\mathbf{U}_k]}$$

$$\mathbf{Y}_{[k]} = \underbrace{\begin{bmatrix} \overline{\mathbf{I}} & \overline{\mathbf{I}} & \overline{\mathbf{0}} \end{bmatrix}}_{[\mathbf{C}]} \underbrace{\begin{bmatrix} \mathbf{X}_{a[k]} \\ \mathbf{X}_{b[k]} \\ \mathbf{X}_{c[k]} \end{bmatrix}}_{[\mathbf{X}_{[k]}]} \tag{13}$$

where $\mathbf{X}_a = [i_{\alpha s} i_{\beta s}]^T$, $\mathbf{X}_b = [i_{xs} i_{ys}]^T$, $\mathbf{X}_c = [i_{\alpha r} i_{\beta r}]^T$, $\mathbf{U}_{\alpha\beta s} = [U_{\alpha s} U_{\beta s}]^T$, $\mathbf{U}_{xys} = [U_{xs} U_{ys}]^T$, $\mathbf{A}$ and $\mathbf{B}$ are matrices that depend on the electrical parameters of the machine and the sampling time $T_m$. Matrix $[\mathbf{A}]$ also depends on the actual value of $\omega_{r[k]}$, which is calculated every sampling time [9].

## B. Rotor state estimation based on Kalman filters

The KF design considers uncorrelated process and zero-mean Gaussian measurement noises, thus the systems equations can be written as:

$$\hat{\mathbf{X}}_{[k+1]} = \mathbf{A}\mathbf{X}_{[k]} + \mathbf{B}\mathbf{U}_{[k]} + \mathbf{H}\varpi_{[k]} \quad (14)$$

$$\mathbf{Y}_{[k+1]} = \mathbf{C}\mathbf{X}_{[k+1]} + \nu_{[k+1]} \quad (15)$$

where $\varpi_{[k]}$ is the process noise, $\mathbf{H}$ is the noise weight matrix and $\nu_{[k+1]}$ is the measurement noise. The dynamics of the KF can be written as follows:

$$\hat{\mathbf{X}}_{c[k+1|k]} = (\mathbf{A}_{33} - \mathbf{K}_{[k]}\mathbf{A}_{13})\hat{\mathbf{X}}_{c[k]} + \mathbf{K}_{[k]}\mathbf{Y}_{[k+1]} + \\ (\mathbf{A}_{31} - \mathbf{K}_{[k]}\mathbf{A}_{11})\mathbf{Y}_{[k]} + (\mathbf{B}_3 - \mathbf{K}_{[k]}\mathbf{B}_1)\mathbf{U}_{\alpha\beta s[k]} \quad (16)$$

being $\mathbf{K}_{[k]}$ the KF gain matrix calculated from the covariance of the noises at each sampling time in a recursive manner as:

$$\mathbf{K}_{[k]} = \mathbf{\Gamma}_{[k]} \cdot \mathbf{C}^T \widehat{R}_\nu^{-1} \quad (17)$$

being $\mathbf{\Gamma}_{[k]}$ the covariance of the new estimation, which it is defined like a function of the old covariance estimation ($\varphi_{[k]}$):

$$\mathbf{\Gamma}_{[k]} = \varphi_{[k]} - \varphi_{[k]} \cdot \mathbf{C}^T(\mathbf{C} \cdot \varphi_{[k]} \cdot \mathbf{C}^T + \widehat{R}_\nu)^{-1} \cdot \mathbf{C} \cdot \varphi_{[k]} \quad (18)$$

From the state equation, it's possible to obtain a correction of the covariance of the estimated state as:

$$\varphi_{[k+1]} = \mathbf{A}\mathbf{\Gamma}_{[k]} \cdot \mathbf{A}^T + \mathbf{H}\widehat{Q}_\varpi \cdot \mathbf{H}^T \quad (19)$$

This completes the required relations for the optimal state estimation using KF with PCC. Thus, $\mathbf{K}_{[k]}$ provides the minimum estimation errors, given a knowledge of the process noise magnitude ($\widehat{Q}_\varpi$), the measurement noise magnitude ($\widehat{R}_\nu$), and the covariance initial condition ($\varphi_{[0]}$).

## C. Speed observer

The speed can be estimated from the dynamic equation that models the mechanical part of the electrical drive (4) and (5) using the Euler discretization method. Thus, the discrete equation which estimates the speed can be written as:

$$\hat{\omega}_{r[k+1]} = (1 - \frac{T_m B_i}{J_i})\hat{\omega}_{r[k]} + \frac{T_m P}{J_i}(T_{e[k]} - T_{L[k]}) \quad (20)$$

where it is assumed $\omega_{r[0]} = 0$, $T_{L[0]} = 0$ and $i_{\alpha\beta r[0]} = 0$.

## D. Load torque observer

The load torque measurement is practically inapplicable, so it must be observed. Hence, it's used the observer based on Gopinath's method proposed in [15], in its discrete version:

$$\begin{bmatrix} \epsilon_{1[k+1]} \\ \epsilon_{2[k+1]} \end{bmatrix} = \begin{bmatrix} 1 & -k_1 T_m \\ T_m & (1 - k_2 T_m) \end{bmatrix} \begin{bmatrix} \epsilon_{1[k]} \\ \epsilon_{2[k]} \end{bmatrix} + \\ T_m \begin{bmatrix} k_1 b J_i \\ (k_2^2 - k_1) J_i \end{bmatrix} \hat{\omega}_{r[k]} + T_m \begin{bmatrix} k_1 \\ k_2 \end{bmatrix} T_{e[k]} \quad (21)$$

$$\hat{T}_{L[k+1]} = \epsilon_{2[k+1]} - k_2 J_i \hat{\omega}_{r[k+1]} \quad (22)$$

where $k_1$, $k_2$ and $b$ are observer coefficients, $\epsilon_1$ and $\epsilon_2$ are internal state variables, $T_e$ is the calculated motor electromagnetic torque and $\hat{T}_L$ is the calculated motor load torque.

## E. Cost function

The cost function should include all terms to be optimized. In current control the most important figure is the tracking error in the predicted stator currents for the next sample. To minimize its magnitude for each sample $k$ it suffices to use:

$$J_{[k+2|k]} = \hat{e}_{i\alpha s[k+2]} + \hat{e}_{i\beta s[k+2]} + \lambda_{xy}\left(\hat{e}_{ixs[k+2]} + \hat{e}_{iys[k+2]}\right) \\ \hat{e}_{i\alpha s[k+2]} = \| i^*_{\alpha s[k+2]} - \hat{i}_{\alpha s[k+2]} \|^2 \\ \hat{e}_{i\beta s[k+2]} = \| i^*_{\beta s[k+2]} - \hat{i}_{\beta s[k+2]} \|^2 \\ \hat{e}_{ixs[k+2]} = \| i^*_{xs[k+2]} - \hat{i}_{xs[k+2]} \|^2 \\ \hat{e}_{iys[k+2]} = \| i^*_{ys[k+2]} - \hat{i}_{ys[k+2]} \|^2 \quad (23)$$

where $\| \cdot \|$ denotes vector magnitude, $i^*_{s[k+2]}$ is a vector containing the reference for the stator currents and $\hat{i}_{s[k+2]}$ is a vector containing the predictions based on the next state (including the delay compensation) and control effort.

## F. Optimizer

The predictive model should be used 64 run to consider all possible voltage vectors. Fig. 2 shows the redundancy of the switching state results in only 49 different vectors (48 active and 1 null). This consideration is commonly known as the optimal solution. For a generic multiphase machine, where $g$ is the number of phase and $\varepsilon$ the search space (49 vectors for the DTPIM), the optimization algorithm produces the optimum gating signal combination $\mathbf{S}^{opt}$ as follows:

---

**Algorithm 1** Proposed algorithm

---

1. **comment:** Optimization algorithm.
2. $J_o := \infty$, $i := 1$
3. **while** $i \leq \varepsilon$ **do**
4.      $\mathbf{S}_i \leftarrow \mathbf{S}_{i,j} \; \forall \, j = 1, ..., g$
5.      **comment:** Compute stator voltages. Eqn. 8.
6.      $U_{\alpha\beta xys} = [u_{\alpha s}\, u_{\beta s}\, u_{xs}\, u_{ys}\, 0\, 0]^T = Vdc \cdot \mathbf{T} \cdot \mathbf{M}$
7.      **comment:** Compute the prediction of the measurement state, considering $\mathbf{X}_{b[0]} = 0$.
8.      $\mathbf{X}_{a[k+1]} = \overline{\mathbf{A}}_{11}\mathbf{X}_{a[k]} + \overline{\mathbf{B}}_1\mathbf{U}_{\alpha\beta s} + \overline{\mathbf{A}}_{12}\mathbf{X}_{b[k]}$
9.      **comment:** Compute the cost function. Eqn. 23.
10.      $J_{[k+2|k]} = \hat{e}_{i\alpha s[k+2]} + \hat{e}_{i\beta s[k+2]} + \lambda_{xy}\left(\hat{e}_{ixs[k+2]} + \hat{e}_{iys[k+2]}\right)$
11.      **if** $J < J_o$ **then**
12.          $J_o \leftarrow J$, $\mathbf{S}^{opt} \leftarrow \mathbf{S}_i$
13.      **end if**
14.      $i := i + 1$
15. **end while**
16. **comment:** Compute the prediction of the unmeasurable state. Eqn. 16.
17. $\hat{\mathbf{X}}_{b[k+1|k]} = (\mathbf{A}_{22} - \mathbf{K}_{[k]}\mathbf{A}_{12})\hat{\mathbf{X}}_{b[k]} + \mathbf{K}_{[k]}\mathbf{Y}_{[k+1]} + (\mathbf{A}_{21} - \mathbf{K}_{[k]}\mathbf{A}_{11})\mathbf{Y}_{[k]} + (\mathbf{B}_2 - \mathbf{K}_{[k]}\mathbf{B}_1)\mathbf{U}_{\alpha\beta s[k]}$
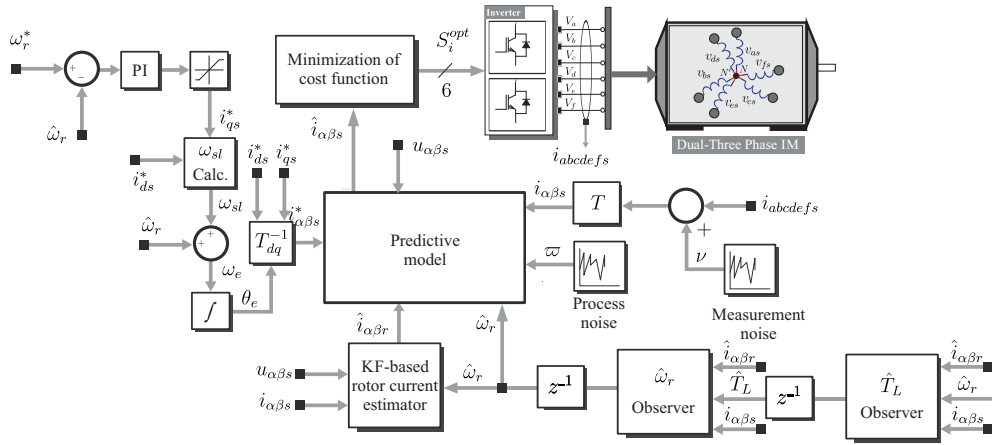
---

Fig. 3. Proposed speed sensorless control technique for the DTPIM.

## G. Proposed predictive control method

From the point of view of the inner loop of the current control, conventional predictive control avoids the use of proportional-integer (PI) controllers and modulation techniques since a single switching vector is applied during the whole switching period. This procedure is somewhat similar to original DTC schemes and leads to variable switching frequency. The proposed control technique selects the control actions by solving an optimization problem for each sampling period. A model of the real system, which is the DTPIM, is used to predict its output. This prediction is carried out for each possible output, or switching vector, of the six-phase inverter to determine which one minimizes a defined cost function, and therefore, the model of the real system, also called predictive model, must be used considering all possible voltage vectors in the six-phase inverter. As the rotor current can not be measured directly, it should be estimated using a KF. The absolute current error, in stationary reference frame $(\alpha - \beta)$ for the next sampling instant is normally used for computational simplicity. In this case, the cost function is defined as (23), where $i^*_{\alpha\beta[k+1]}$ is the stator reference current and $i_{\alpha\beta[k+2]}$ is the predicted stator current which is computationally obtained using the predictive model. Proportional integral (PI) controller with saturator is used in the speed sensorless control loop, based on the indirect vector control scheme because of its simplicity. In the indirect vector control scheme, PI speed controller is used to generate the reference current $i^*_{qs}$ in dynamic reference frame. The current reference used by the predictive model are obtained from the calculation of the electric angle used to convert the current reference, originally in dynamic reference frame $(d - q)$, to static reference frame $(\alpha - \beta)$. The process of calculation of the slip frequency $(\omega_{sl})$ is performed in the same manner as the Indirect Field Orientation methods, from the reference currents in dynamic reference frame $(i^*_{ds}, i^*_{qs})$ and the electrical parameters of the machine $(R_r, L_r)$. Finally, using the rotor current estimated, the stator current measured and the load torque measured from the induction machine we can estimate

TABLE I
PARAMETERS OF THE DTPIM

| PARAMETER | Dual three-phase induction machine | | |
| --- | --- | --- | --- |
| | SYMBOL | VALUE | UNIT |
| Stator resistance | $R_s$ | 12.8 | $\Omega$ |
| Rotor resistance | $R_r$ | 4.79 | $\Omega$ |
| Stator leakage inductance | $L_{ls}$ | 77.92 | mH |
| Stator inductance | $L_s$ | 897.97 | mH |
| Rotor inductance | $L_r$ | 897.97 | mH |
| Magnetizing inductance | $L_m$ | 818.05 | mH |
| System inertia | $J_i$ | 0.02 | kg.m$^2$ |
| Pairs of poles | $P$ | 3 | $-$ |
| Friction coefficient | $B_i$ | 0.036 | kg.m$^2$/s |
| Nominal frequency | $f_a$ | 50 | Hz |
| Electrical power | $P_w$ | 15 | kW |

the speed of the machine. A detailed block diagram of the proposed sensorless speed control technique for the DTPIM drive is provided in Fig. 3.

## V. SIMULATION RESULTS

A MATLAB/Simulink simulation environment has been designed for the VSI-fed DTPIM, and simulations have been performed to show the efficiency of the proposed predictive speed control technique. Numerical integration using first order Euler's method algorithm has been applied to compute the evolution of the state variables step by step in the time domain. Table I shows the electrical and mechanical parameters for the DTPIM. The efficiency of the proposed speed sensorless control algorithm for the DTPIM has been evaluated, under load conditions. In all cases is considered a sampling frequency of 10 kHz. Fig. 4 shows the simulation results for a multi-step speed references [180, 220, -220, -180] rpm, if we consider a fixed reference current ($i^*_{ds} = 1$ A). The subscripts $(\alpha - \beta)$ represent quantities in the stationary frame reference of the stator currents. The estimated speed is fedback into the closed loop for speed regulation and a PI controller is used in the speed regulation loop as shown in Fig. 3. Furthermore, it can be seen from this graph (as zoom),
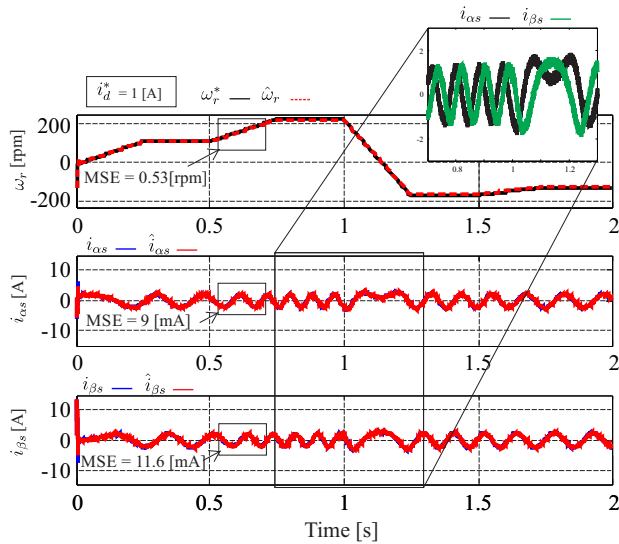
Fig. 4. Simulation results for a multi-step speed references application.



Fig. 5. Simulation results for a multi-step load torque application.

the change in the phases of the stator currents in the $(\alpha - \beta)$ subspace, caused by the reversal of the direction of rotation of the machine. Under these test conditions, the mean squared error (MSE) in the speed and current tracking are 0.53 rpm, 9 mA and 11.6 mA, respectively.

Fig. 5 shows a multi-step load torque application response [15, 30, -30, -15] N·m, and the rotor current evolution (measured and observed) in a stationary reference frame. It can be seen in this graph the amplitude variation of the rotor current in function to the load torque applied to the machine. The estimated rotor current converges to real values for these test conditions as shown in figures, considering that the MSE is 98 mA and 99 mA for $i_{\alpha r}$ and $i_{\beta r}$, respectively.

## VI. CONCLUSION

In this paper, the propulsion drive of EVs based in a sensorless speed control scheme of a DTPIM using an inner loop based on the MPC control is proposed. The MPC is designed through a state-space representation, where the rotor and stator current are the state variables. The rotor current is estimated using a KF. The theoretical development of the controller has been validated through simulation results. The method avoids the use of a speed sensor and has proven to be efficient even when considering that the machine is operating under varying speeds and load regimes.

## ACKNOWLEDGMENT

## REFERENCES

[1] M. J. Duran and F. Barrero, "Recent advances in the design, modeling, and control of multiphase machines: Part I," *IEEE Trans. Ind. Electron.*, vol. 63, no. 1, pp. 459–468, 2016.
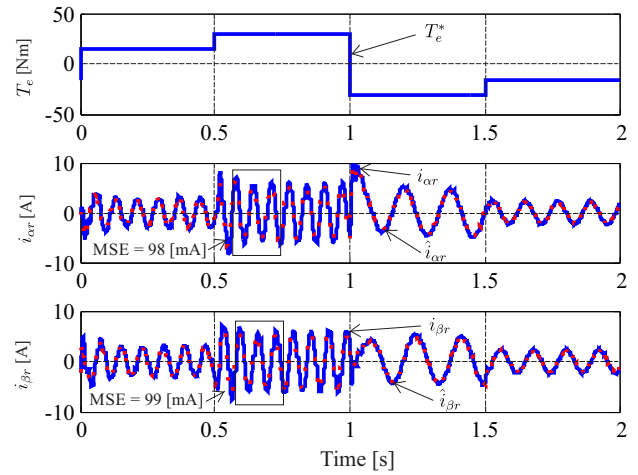
[2] J. Riveros, B. Bogado, J. Prieto, F. Barrero, S. Toral, and M. Jones, "Multiphase machines in propulsion drives of electric vehicles," in *Proc. EPE/PEMC*, 2010, pp. T5–201.

[3] M. Villani, M. Tursini, G. Fabri, and L. Castellini, "High reliability permanent magnet brushless motor drive for aircraft application," *IEEE Trans. Ind. Electron.*, vol. 59, no. 5, pp. 2073–2081, 2012.

[4] L. Jin, S. Norrga, H. Zhang, and O. Wallmark, "Evaluation of a multiphase drive system in ev and hev applications," in *Proc. IEMDC*. IEEE, 2015, pp. 941–945.

[5] R. Gregor and J. Rodas, "Speed sensorless control of dual three-phase induction machine based on a luenberger observer for rotor current estimation," in *Proc. IECON*, 2012, pp. 3653–3658.

[6] A. Taheri and M. Mohammadbeigi, "Speed sensor-less estimation and predictive control of six-phase induction motor using extended kalman filter," in *Proc. PEDSTC*, 2014, pp. 13–18.

[7] F. Wang, X. Mei, H. Dai, S. Yu, and P. He, "Sensorless finite control set predictive current control for an induction machine," in *Proc. ICIA*, 2015, pp. 3106–3111.

[8] A. S. Morsy, A. Abdel-Khalik, S. Ahmed, and A. Massoud, "Sensorless field oriented control of five-phase induction machine under open-circuit phase faults," in *Proc. ECCE*, 2013, pp. 5112–5117.

[9] J. Rodas, F. Barrero, M. R. Arahal, C. Martin, and R. Gregor, "On-line estimation of rotor variables in predictive current controllers: A case study using five-phase induction machines," 2016.

[10] L. Zhao, J. Huang, H. Liu, B. Li, and W. Kong, "Second-order sliding-mode observer with online parameter identification for sensorless induction motor drives," *IEEE Trans. Ind. Electron.*, vol. 61, no. 10, pp. 5280–5289, 2014.

[11] M. Comanescu, "Design and implementation of a highly robust sensorless sliding mode observer for the flux magnitude of the induction motor," *IEEE Trans. Energy Convers.*, vol. 31, no. 2, pp. 649–657, 2016.

[12] R. Gregor, J. Rodas, J. Munoz, M. Ayala, O. Gonzalez, and D. Gregor, "Predictive-fixed switching frequency technique for 5-phase induction motor drives," in *Proc. SPEEDAM*, 2016.

[13] Y. Zhao and T. A. Lipo, "Space vector PWM control of dual three-phase induction machine using vector space decomposition," *IEEE Trans. Ind. Electron.*, vol. 31, no. 5, pp. 1100–1109, 1995.

[14] H. S. Che and W. P. Hew, "Dual three-phase operation of single neutral symmetrical six-phase machine for improved performance," in *Proc. IECON*, 2015, pp. 001 176–001 181.

[15] J. Guzinski, H. Abu-Rub, M. Diguet, Z. Krzeminski, and A. Lewicki, "Speed and load torque observer application in high-speed train electric drive," *IEEE Transactions on Industrial Electronics*, vol. 57, no. 2, pp. 565–574, 2010.